ISSN 2070-0482, Mathematical Models and Computer Simulations, 2024, Vol. 16, No. 1, pp. 63–75. © Pleiades Publishing, Ltd., 2024.
Russian Text © The Author(s), 2023, published in Matematicheskoe Modelirovanie, 2023, Vol. 35, No. 9, pp. 96–116.

Application of the Harmonic Balance Method to Calculate the First Booster Stage Tonal Noise

A. A. Rossikhin[a],* and V. I. Mileshin[a]

[a] *Baranov Central Institute of Aviation Motors, Moscow, 111116 Russia*

**e-mail: aarossikhin@ciam.ru*

Received April 10, 2023; revised May 22, 2023; accepted July 3, 2023

Abstract—The results of the numerical investigation of the tone noise of the first booster stage of a high bypass ratio turbofan in the far field in the approach (landing) operational conditions are presented. The study is performed using the frequency domain numerical method of multistage turbomachines tonal noise simulation, developed at the Baranov Central Institute of Aviation Motors (CIAM). A variant of the method suitable for the calculations in a nonlinear setup is used. The calculation is performed for several blade passages in each row. The harmonic balance method for multitonal disturbances with a frequency mapping is implemented. The results of the calculations are compared with the results of the calculations in the time domain, presented in the previous paper (they were also performed in a nonlinear setup) and with the experimental data obtained at the CIAM acoustic test facility. In general, satisfactory correspondence is found between the data in both cases. The results can be treated as an argument for the validity of the proposed nonlinear frequency domain method of the multistage turbomachinery tone noise calculations.

Keywords: booster stage noise, multistage turbomachine noise, tonal noise, computational aeroacoustics, frequency domain calculation methods, harmonic balance method, frequency mapping

DOI: 10.1134/S2070048224010083

1. INTRODUCTION

One of the components of the tonal noise of a turbojet engine is the interaction noise between the rows in the booster stages of the low-pressure compressor. Although booster stages are much less significant as a noise source than a fan, their noise can be noticeable in some engine operating modes [1, 2].

The peculiarity of retaining stages as a source of noise compared to a fan is that their noise is usually determined by the interaction of several rows. For example, in the process of calculating the noise of the first booster stage in the front hemisphere, it is necessary to take into account the interactions of the stage impeller both with the input guide vane of the booster stages and with the stage guide vane. It is also necessary to take into account the interaction of stage noise with the fan impeller.

The simplest approach to calculate the tonal noise of a multistage turbomachine in terms of formulation is a direct nonstationary calculation in all impeller passages of each row. However, it is very expensive in terms of computing resources. Therefore, it seems natural to use frequency domain methods that have proven to be computationally efficient when applied to fan tonal noise calculations. Moreover, such methods for calculating the noise of multistage blade machines have indeed been developed. Examples can be found in [1, 3, 4].

In the process of studying the tonal noise of the booster stages at the Central Institute of Aviation Motors (CIAM), a method was developed for calculating the noise of multistage turbomachines in the frequency domain [5, 6]. In this method, the pulsations in the rows are calculated in a linear approximation. The solution in the blade row is sought in the form of a set of fields of harmonic fragments in one interscapular passage of the row. The concept of a harmonic fragment—a set of disturbances in a row having the same frequency and phase shift between the boundaries of the interscapular passage—was presented in [5]. In this study, it is shown that the flow in the row can be decomposed into harmonic fragments, and for each of the harmonics of the base frequency of disturbances in the row of the turbomachine, there is only a finite number of harmonic fragments, determined by the geometry of the turbomachine. Taking into account in the calculation only those harmonic fragments that correspond to the strongest compensations generated in the turbomachine, the need for computing resources can be significantly reduced.

As a validation problem for the calculation method, we used the problem of calculating the noise of the first booster stage of a low-pressure compressor (LPC) in the far field, taking into account the passage of noise through the fan impeller. The paper [6] presents the calculation of tonal noise for a mode with a relatively reduced rpm of $N = 53.9\%$ (the landing mode); and [7], also at a rpm of $N = 75.5\%$. Both works show that the calculation results are close to the experimental results obtained at the CIAM stand. It is also worth mentioning the work [8], in which the tonal noise of three supporting stages was calculated, and entirely satisfactory agreement was found between the calculation and experiment.

To further verify the calculation method in [9], the tonal noise of the same first booster stage was calculated using a time domain calculation method. The calculation was performed in a nonlinear formulation. Satisfactory agreement between the calculation results in the time and frequency domains is shown.

Work [10] describes a generalization of the method proposed in [5, 6] to the case of calculation in a nonlinear formulation using the harmonic balance method. It was shown that the calculation of the generation and propagation of noise in a multistage turbomachine using the harmonic balance method can be carried out in a computational domain that includes only several impeller passages in each row of the turbomachine. A similar approach, in which the calculation is carried out in a computational domain that is reduced in the circumferential direction, was previously proposed in the time domain calculation method in [11, 12].

The method described in [10] is used in this study to calculate the tonal noise of the first supporting stage, previously studied in [6–9]. The calculation results are compared with the results of calculations in the time domain, as well as with the experimental data. Although previous works did not reveal significant differences between the calculation results in different formulations, this study made it possible to test the method on a real three-dimensional problem and demonstrate its performance.

In [10], good conditionality of the matrices used to convert the data from the time domain to the frequency domain in the harmonic balance method was ensured by selecting the moments of time at which the fluxes were calculated using special algorithms. A feature of this work is the use of the harmonic balance method for multitonal disturbances, based on an artificial frequency mapping [13]. This approach appears to have been rarely used in gas dynamic calculations. However, the significant simplification of the calculation procedure provided by this method persuaded the authors to make this choice.

2. EULER EQUATIONS FOR DISTURBANCES

The numerical method used in this study is based on the use of linear or nonlinear Euler equations for disturbances over the average stationary flow field in the blade rows. These equations are obtained by separating the flow parameters $\mathbf{U} = (\rho, \rho u, \rho v, \rho w, e)$ in the Euler equations in a conservative form for the stationary flow field (indicated by index 0) and the pulsation field (indicated by the prime) and subtracting from the resulting equations the parts that describe only the average flow field. In the reference system rotating with angular velocity Ω around axis x, these equations can be written [14–16] in the form

$$\partial \mathbf{U}'/\partial t + \mathbf{R}'(\mathbf{U}_0, \mathbf{U}') = 0, \tag{1}$$

where

$$\mathbf{R}' = \partial \mathbf{E}'/\partial x + \partial\left[\mathbf{F}' - \Omega z \mathbf{U}'\right]/\partial y + \partial\left[\mathbf{G}' + \Omega y \mathbf{U}'\right]/\partial z - \mathbf{S}'; \tag{2}$$

$\mathbf{U}'$ is the disturbance vector; $\mathbf{U}_0$ is the vector of the average flow field; $\mathbf{E}'$, $\mathbf{F}'$, and $\mathbf{G}'$ are flow vectors for disturbances; and $\mathbf{S}'$ is the source required to describe the rotation effect, $\mathbf{S}' = (0, 0, \Omega U_4', -\Omega U_3', 0)$. In the numerical method used, Eqs. (1) and (2) can be considered both in a linear approximation and contain nonlinear terms.

3. HARMONIC BALANCE METHOD

In the case when the disturbance under study can be characterized by a finite set of frequencies, the nonstationary problem can be reduced to a set of stationary ones. Let us imagine vectors at each point of the computational domain $\mathbf{U}'$ and $\mathbf{R}'$ as

$$\mathbf{U}'(x, y, z, t) = \sum_{k=-N_h}^{N_h} \mathbf{U}_{h_k}'(x, y, z) \exp(-i\omega h_k t), \tag{3}$$

$$\mathbf{R}'(x,y,z,t) = \sum_{k=-N_h}^{N_h} \mathbf{R}'_{h_k}(x,y,z)\exp(-i\omega h_k t), \tag{4}$$

where h is the harmonic number of the base frequency, ω is the base frequency, and $h_{-k} = -h_k$.

Substituting (3) and (4) into (1), we can obtain a set of systems of equations for harmonic fields

$$-i\omega h_k \mathbf{U}'_{h_k} + \mathbf{R}'_{h_k} = 0. \tag{5}$$

Since the flow field is real, $\mathbf{U}'_{-h}(x,y,z) = \mathbf{U}'^{*}_{h}(x,y,z)$ and, therefore, there are only N_h complex systems of equations and one real system of equations (for harmonics with zero frequency).

To close Eq. (5), it is necessary to express $\mathbf{R}'_h$ through a set of variables $\{\mathbf{U}'_{h_s}\}$, $-N_h \le s \le N_h$. If Eq. (2) is linear, $\mathbf{R}'_h$ is easily expressed in terms of complex harmonic amplitudes [16]. In the nonlinear case, the harmonic balance method is usually used to solve the problem [17]. The Fourier transform (3) is used to reconstruct unsteady flow fields for the given set of times $\{t_k\}$. After this the values $\mathbf{R}'$ are calculated at the given times. Then the inverse transformation to (4) is used to calculate $\mathbf{R}'_h$.

To solve the resulting system of equations (5), in the numerical method under consideration, the pseudo-time setting method is used. In this case, a local time step is used to accelerate convergence. Iteration over time is carried out using the Runge–Kutta method.

4. ARTIFICIAL FREQUENCY MAPPING METHOD

It is usually more convenient to describe noise in a multistage turbomachine not by one tone and several of its harmonics but by a combination of several tones and their harmonics. In the case of a multitone harmonic balance, the construction of a transformation matrix from fields in the time domain to a set of harmonic fields becomes significantly more complicated compared to a single-tone balance. As a rule, the transformation matrix is constructed numerically, and significant efforts have to be made when choosing $\{t_k\}$ in order for this matrix to be acceptably conditioned [13].

The frequency mapping method is a popular approach to solve multitone harmonic balance problems. It is based on two observations. Firstly, when carrying out the calculation, it is necessary to calculate only the spectrum of the vector $\mathbf{R}'(\mathbf{U}'(t))$ using the spectrum $\mathbf{U}'(t)$; i.e., the time domain representation of these two vectors is not important. Secondly, the coefficients of the Fourier series expansion for the vector $\mathbf{R}'(\mathbf{U}'(t))$ do not depend on the frequencies that characterize the vector $\mathbf{U}'(t)$ [13]. We assume in the calculation problem that the set of frequencies that describes the disturbances contains N_h harmonics with a positive frequency. Then, according to what has been said, when using the harmonic balance method, this set of frequencies can be replaced by some artificial set of frequencies, which represents the first N_h harmonics of some basic frequency. For such a set of harmonics, the construction of a matrix for the direct and inverse Fourier transforms is significantly simplified.

The specific form of the display depends on the set of source frequencies being considered. In [13] we can find different mappings associated with different ways of choosing the initial frequencies. In this study we will consider disturbances whose frequencies are combinations of two frequencies, ω_1 and ω_2. The number of frequencies in the set will be limited by the intermodulation order $K_{\max}$. This value determines the permissible frequencies as follows: they can take values corresponding to the formula

$$\omega = a\,\omega_1 + b\,\omega_2, \quad |a| + |b| \le K_{\max}, \quad a,b \in \mathbb{Z}. \tag{6}$$

The number of allowed frequencies M with a positive frequency is determined by the relation $M = K_{\max}(K_{\max}+1)$. With this choice of the frequencies under consideration, the frequencies are displayed as follows:

$$\omega_1 = K_{\max}\lambda_0, \quad \omega_2 = (K_{\max}+1)\lambda_0,$$

where λ_0 is some arbitrary positive real number. It is easy to show that in this case the frequencies from set (6) are mapped into the set defined by the relation $\omega' = p\lambda_0$, $p = 0, \ldots, M$. Constructing direct and inverse Fourier transforms for such a set of frequencies is trivial.

5. METHOD FOR CALCULATING THE NOISE OF A MULTISTAGE TURBOMACHINE

This section describes the method for calculating the tonal noise of the multistage turbomachine used in this study. The method is based on kinematic relations describing the dependence of flow fields in a turbomachine on time and the azimuthal angle, described earlier in [5, 6, 8, 10].

We assume that the turbomachine contains two groups of rows: stationary stator rows and rotor rows rotating at a peripheral velocity Ω. The flow fields can be considered both in the reference system of one group of rows and in the reference system of the other one. The belonging of physical quantities to one or another group of rows will be indicated by a superscript. The index values for the stator rows are set to 1; and for rotor rows, to 2. In the case where the value of the index is not specified, it is denoted by a capital Latin letters. Two letters are used in a special way: index A denotes the group of rows in whose reference system the field is considered; and B, the other group of rows.

Let us denote by B_μ^C the number of blades in the μth row in the Cth group. The spectrum of disturbances in a turbomachine is determined by the greatest common divisors of the numbers of blades of groups: $P^1 = gcd(B_1^1, ..., B_{N1}^1)$ and $P^2 = gcd(B_1^2, ..., B_{N2}^2)$. It can be shown [5] that the expression for the disturbance of the flow field $\mathbf{U}'$ in the flow path of a turbomachine in the reference system of the group of rows A can be written as a superposition of components (azimuthal modes) of the form

$$\mathbf{U}'_{j^A j^B}(x,r,\theta^A,t) = \mathbf{U}'_{j^A j^B}(x,r)\exp(im\theta^A - i\omega^A t),$$
$$m = j^A + j^B, \quad \omega^A = j^B\Omega^{AB}, \tag{7}$$

where t, x, r, and θ^A are the time and cylindrical coordinates in the reference system associated with row A. It is assumed that the second, third, and fourth components of $\mathbf{U}'$ correspond to the components of the mass flow pulsation vector, written in the cylindrical coordinate system, where

$$j^A = \sum_{\mu=1}^{N^A} j_\mu^A B_\mu^A = P^A h^A, \quad j^B = \sum_{\mu=1}^{N^B} j_\mu^B B_\mu^B = P^B h^B. \tag{8}$$

Here, j_μ^C and h^C are arbitrary integers. Equation (8) is a consequence of the known properties of Diophantine equations. Thus, the basic frequencies of tonal noise in the stator and rotor reference frames are equal, respectively, to $P^2\Omega^{12}$ and $P^1\Omega^{21}$. Here $\Omega^{12} = \Omega$ denotes the rotor velocity relative to the stator; and $\Omega^{21} = -\Omega$, the stator's rotation frequency relative to the rotor.

The flow field in a turbomachine can be decomposed in each of the rows into harmonics of the base frequency for this row. For the μth row in the group of rows A, the corresponding expansion for the vector of conservative variables has the form

$$\mathbf{U}'^A_\mu(t,x,r,\theta^A) = \sum_{h^B=-\infty}^{\infty} \mathbf{U}'^A_{\mu h^B}(x,r,\theta^A)\exp(-iP^B\Omega^{AB}h^B t). \tag{9}$$

For a multistage turbomachine, the computational domain for the fields of complex harmonic amplitudes in the row generally cannot be reduced to a single impeller passage (unlike a single-stage turbomachine). The minimum size of the computational area by angle is a sector with a dimension of $2\pi/P^A$ radians containing interscapular passages for the given interscapular row $Q_\mu^A = B_\mu^A/P^A$.

In [5, 6] it was shown that harmonic fields can be decomposed into components, whose domain of definition is limited to one interscapular passage. They can be characterized as the set of disturbances in the row that has the same phase shift and frequency in the reference frame of the given row. In total there is a row for each frequency Q_μ^A of harmonic fragments. Let us denote by θ_{bb} the angular coordinate, which describes the position of a point inside the interscapular passage and is related to the angular coordinate in the row by the relation $\theta^A = \theta_{bb} + 2\pi/B_\mu^A n$, where n is the number of the interscapular passage, counted from zero. According to [6]:

$$\mathbf{U}'^A_{\mu h^B}(x,r,\theta^A) = \sum_{q=0}^{Q_\mu^A-1} \mathbf{F}'^A_{\mu h^B q}(x,r,\theta_{bb})\exp\left(i2\pi n[q/Q_\mu^A + P^B h^B/B_\mu^A]\right), \tag{10}$$

$$\mathbf{F}'^{A}_{\mu h^{B} q}(x, r, \theta^{+}_{bb}) = \mathbf{F}'^{A}_{\mu h^{B} q}(x, r, \theta^{-}_{bb}) \exp\left(i 2\pi [q/Q^{A}_{\mu} + P^{B} h^{B}/B^{A}_{\mu}]\right). \quad (11)$$

Here, $\mathbf{F}'^{A}_{\mu h^{B} q}(x, r, \theta_{bb})$ is the vector of conservative variables for a harmonic fragment, defined in one impeller passage. Surfaces $\theta^{+}_{bb}(x, r)$ and $\theta^{-}_{bb}(x, r)$ determine the boundaries of the zero impeller passage (for it, $\theta^{-}_{bb} \le \theta_{bb} \le \theta^{+}_{bb}$).

Frequency domain calculation methods are based on the assumption that the flow field in a row can be characterized by a finite (and rather small) number of harmonics N^{C}_{h}. The considered method for calculating the tonal noise of multistage turbomachines is based on the assumption [5, 6] that the flow in the row can be characterized by a small number of harmonic fragments N^{C}_{f}. Substituting expansion (10) into (5), we can get

$$-i\omega h_{k} \mathbf{F}'^{A}_{\mu h^{B}_{k} q_{k}} + \mathbf{R}'^{A}_{\mu h^{B}_{k} q_{k}}(\mathbf{F}') = 0. \quad (12)$$

To close Eq. (12), it is necessary to express $\mathbf{R}'^{A}_{\mu h^{B} q}$ through a set of variables $\{\mathbf{F}'^{A}_{\mu h^{B} q}\}$. In the linear case, the equations for different harmonic fragments are independent, which is what the calculations in [5–8] were based on. In the nonlinear case, to solve the problem, as before, we can use the harmonic balance method. In this case, instead of transforming (3) from a set of harmonic fields to a set of fields for moments of time $\{t_k\}$ and its inverse, we should use transformation (9), (10) from a set of fields of harmonic fragments to a set of fields for the given pairs of moments of time and impeller passages $\{t_k, n_k\}$ and the corresponding inverse transformation. The disadvantage of this approach is the complexity of constructing a well-conditioned transformation matrix and the high computational cost of converting from one data representation to another.

Another approach to calculate the flow field in blade machines using the harmonic balance method was proposed in [10]. If the flow field for some harmonic h_k can be described by N^{k}_{f} harmonic fragments, then in order to calculate these harmonic fragments, it is sufficient to know the flow field only in N^{k}_{f} interscapular passages. Therefore, the calculation of fields for N^{k}_{f} harmonic fragments can be reduced to the calculation of fields of complex amplitudes for harmonics h_k, specified in the computational domain, including N^{k}_{f} interscapular passages. In this case, special boundary conditions must be used at the boundaries of the computational domain. We assume that the passages are arranged in ascending order n from 0 to $N^{k}_{f} - 1$. Then the boundary conditions at the outer boundaries of the computational domain, corresponding to the periodic boundaries of the impeller passages, can be specified based on the data on the flow fields at the periodic boundaries of the impeller passages inside the computational domain. According to [10],

$$\mathbf{U}'^{A}_{\mu h^{B}_{k}}\left(x, r, \theta^{+}_{bb} + 2\pi(N^{k}_{f} - 1)/B^{A}_{\mu}\right) = \sum_{j=0}^{N^{k}_{f}-1} S^{j}_{\mu h^{B}_{k}} \mathbf{U}'^{A}_{\mu h^{B}_{k}}\left(x, r, \theta^{-}_{bb} + j\, 2\pi/B^{A}_{\mu}\right), \quad (13)$$

where the coefficient values $S^{j}_{\mu h^{B}_{k}}$ can be obtained from Eq. (10) and depend only on the harmonic number and the given set of harmonic fragments. If the number of impeller passages is the same for all the considered harmonics, the standard harmonic balance method can be used for calculations in a nonlinear formulation.

The advantage of this method is that calculations in a nonlinear formulation using the harmonic balance method are much simpler to set up and require less computational resources than calculations using the method based on Eq. (12). Therefore, it will be used in this study.

6. GENERAL CHARACTERISTICS OF THE METHOD FOR CALCULATING THE TONAL NOISE OF BLADE MACHINES

The input data for the tonal noise calculation method are a stationary flow field in the computational domain and a curvilinear multiblock computational grid consistent with the boundaries of the computational domain. The average steady-state flow field in the row of the turbomachine must be obtained using a solver for the Reynolds-averaged Navier–Stokes equations, using a finite-volume mesh and a boundary

condition such as a mixing surface between the rows (the use of viscous equations is necessary to resolve the traces). The obtained results are used as the input data for nonstationary calculations. It can be performed in both the time and frequency domains.

The finite volume method is used for spatial discretization. To approximate the flows, a fourth-order dispersion relation preserving (DRP) scheme is used [18], rewritten for a curvilinear coordinate system (additional details can be found in [15]). Various Runge–Kutta schemes can be used for integration by time in the numerical method. In this study, fourth-order Runge–Kutta schemes of the highly accurate large-step explicit Runge–Kutta (HALE-RK) type were used [19].

To suppress high-frequency parasitic disturbances, artificial viscosity with an 11-point pattern was introduced in the scheme. In the nonlinear case, adaptive viscosity is used. Following [20], pressure is used to detect large flow field gradients.

In the developed method, several types of boundary conditions are used at the boundaries of the blocks that make up the computational grid. On solid surfaces, nonflow conditions are specified. The introduction and removal of disturbances from the computational domain is described using the one-dimensional characteristic boundary conditions [21].

The boundaries between blocks are set by copying the flow parameters from the boundary cells into the corresponding "foreign" cells of the neighboring blocks. At periodic boundaries, in addition to transferring the data to the corresponding boundary cells of the conjugate boundary, the velocity vector is rotated by the angle of periodicity. When calculating in the frequency domain, additional phase shifts for flow parameters can be introduced at these boundaries according to formula (11). The boundary conditions for the boundary of the computational domain with several impeller passages are described by formula (13).

The interaction between computational domains for adjacent rows in the time domain is carried out using interfaces of the sliding grid type. The complete flow parameters are interpolated from the boundary cells of one computational domain to the foreign cells of another at each step of the Runge–Kutta scheme. The interpolated flow parameters, together with the parameters of the average flow field, are used to calculate the flows generated by unsteady disturbances. If the calculation is carried out in the frequency domain, the parameters are transferred between the rows for a predetermined set of azimuthal modes of the total flow field at each iteration. When constructing these boundary conditions, the formalism of the harmonic fragments is used (the details can be found in [6]).

A semianalytical technique based on the Fox Williams–Hawkings equation is used to calculate the far-field radiation [22].

7. OBJECT OF STUDY

The considered low-pressure compressor in the bench configuration is a model with a diameter of $D =$ 700 mm. The model includes a fan with wide-chord impeller blades, designed for a promising civil aircraft engine, as well as three supporting stages. A description of the model can be found in [6–8] and the references given there.

The model has $B_1^2 = 18$ blades in the fan impeller (FI), $B_1^1 = 71$ blades in the inlet guide vane (IGV_I) of the booster stages, $B_2^2 = 86$ blades in the impeller of the first booster stage (FI_I), and $B_2^1 = 100$ blades in the guide vane of the first booster stage (GV_I). The data on the other two rows can be found in [8]. The model diagram is shown in Fig. 1.

This paper studies the calculation of the tonal noise of the first booster stage, taking into account the effects caused by the passage of noise through the fan impeller. The calculations were performed for the subsonic landing mode at the corresponding relative shaft rotation frequency $N = 53.9\%$. The bypass ratio for this operating mode is 9.7, the peripheral velocity of the fan impeller is 212.9 m/s, and the peripheral velocity of the first booster stage impeller is 119.4 m/s. For comparison, at the design point, the bypass ratio is 8.5, the peripheral velocity of the fan impeller is 395 m/s, and the peripheral velocity of the first booster stage impeller is 221.5 m/s. A feature of the landing mode is that for it the noise of the booster stage prevails in the front hemisphere over the noise of the fan [7].

The results of the experiment [6, 7] show that the main contribution to the noise of the booster stages is made by tones whose frequencies are combinations of the blade repetition frequency (BRF) of the impeller of the booster stage, $f_2 = B_2^2\Omega/2\pi$, and the frequencies of some BRF harmonics of the fan impeller $f_1 = B_1^2\Omega/2\pi$. The calculations performed by the authors earlier showed that the noise at these frequen-

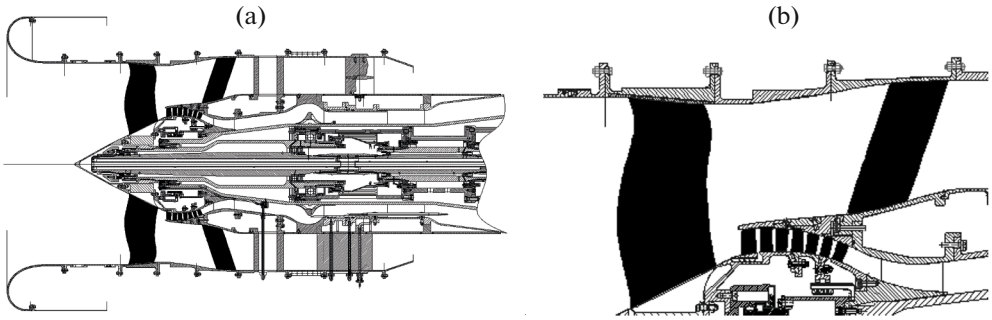

Fig. 1. Scheme of the model LPC: (a) general view, (b) enlarged fragment.

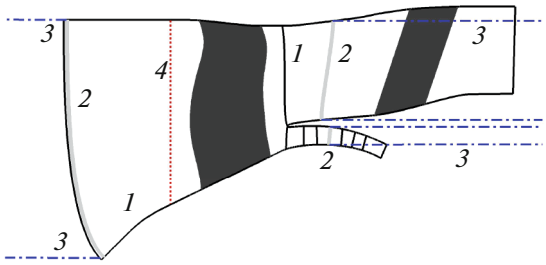

Fig. 2. Scheme of the computational domain. Here, (*1*) are boundaries of the blocks of the original grid; (*2*) are boundaries of the detailed grid area in calculations performed using harmonic methods; (*3*) are boundaries of buffer blocks (only partially shown); (*4*) is the surface for modal analysis.

cies is generated predominantly as a result of the scattering of the azimuthal modes with the frequency equal to the BRF of the stage impeller on the fan impeller. Therefore, our first priority was to correctly describe the noise generation mechanisms of the noise stage at this frequency, as well as at frequencies of $f_2 - f_1$ and $f_2 + f_1$.

8. PREPARATORY OPERATIONS

The stationary flow field in the model fan and booster stages were calculated at the first stage of this study. The calculation was carried out using the Navier–Stokes equations, a semiempirical turbulence model, and mixing-plane-type interfaces between rows. For the calculation, one of the CIAM calculation methods was used [15].

To perform the calculations, a multiblock finite-volume mesh with *N*-topology, covering one impeller passage for the FI, one impeller passage for the straightening apparatus (SA) in the outer contour, and one impeller passage for each of the rows of the booster stages. The mesh is denser towards the boundaries of the hard surface type, as well as near the leading and trailing edges of the blades. The size of the computational grid is 5.6 million cells. The diagram of the computational domain is shown in Fig. 2 with black curves. The meridional projections of the rotor and stator blades are shown in dark gray (for the other rows, the projections are not shown so as not to clutter the diagram). The calculation was performed under the standard inlet conditions: $P^* = 101\,325$ Pa and $T^* = 288.15$ K. The radial equilibrium condition is specified in the exit section. The boundary condition at the outlet of the internal loop is set in the form of the given value of the mass air flow.

The results of calculations for the relative Mach number showed that the flow for the 53.9% regime is subsonic throughout the entire computational region. The obtained values for the integral gasdynamic characteristics of the low-pressure compressor are close to the corresponding measurement results at the CIAM stand.

The computational area for the unsteady calculations includes an area containing a fan impeller blade, areas containing IGV_I, FI_I, and GV_I blades, as well as the area containing the entrance to the outer loop. The region containing the SA was excluded from the calculation domain, since in this study, attention was

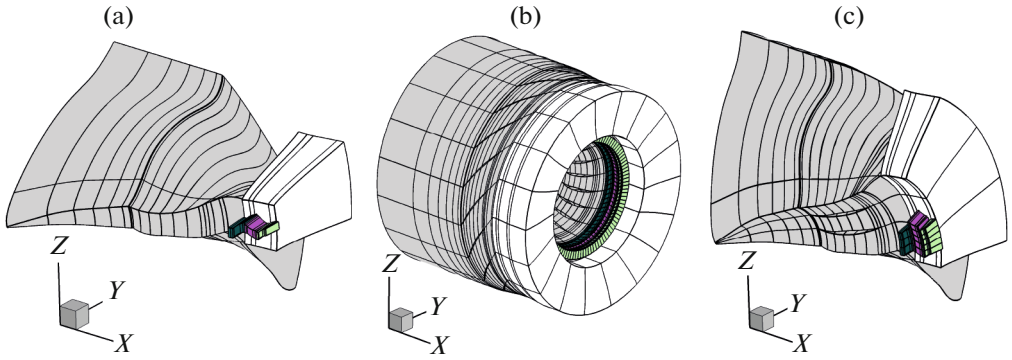

Fig. 3. Computational domains for calculations in different formulations: (a) calculation in the frequency domain in a linear formulation; (b) calculation in the time domain; (c) nonlinear calculation in the frequency domain. Black curves are block boundaries.

focused on calculating the noise in the front hemisphere. It was decided to neglect the process of reflection of the noise from the stator.

The grid used in the nonstationary calculation was reconstructed from the grid for the stationary calculation. For ease of parallelization, the grid was divided into a larger number of blocks. The x-coordinate grid size in the FI was increased to ensure that the high-frequency disturbances generated by the propagation stage propagate without a significant error. From the blocks related to the SA, only a part of the grid remained, corresponding to the entrance to the outer contour. It was changed so that its angular size coincided with the angular size of the part of the mesh containing the FI. In addition, the flow in it was averaged over the azimuthal angle in order to remove the inhomogeneities related to the presence of the SA. This made it possible to then set a rotation velocity for this area equal to the shaft rotation velocity, and carry out calculations in it for the same harmonics as in the FI.

At the last stage of reconstruction, buffer blocks were added to the resulting computational meshes to prevent nonphysical reflections from the boundaries. A schematic representation of the computational domain for calculating interaction noise (and for the stationary calculation) is shown in Fig. 2. The light gray lines show the boundaries of the detailed grid, and the dashed-dotted lines show the boundaries of the buffer blocks.

The total grid size was 4.2 million cells. In the blocks related to the FI and the entrance to the external contour, there were 3.27 million cells; in the blocks related to the IGV_I, 0.23 million cells; in the blocks related to FI_I, 0.28 million cells; and in the blocks related to GV_I, 0.42 million cells. The dominance of blocks related to the FI is clear from a comparison of the blade sizes. The computational area included 74 blocks.

9. SUMMARY OF PREVIOUS STUDIES

For the object studied in this paper, tonal noise calculations were previously performed using two different methods. The calculations presented in [6, 7] were carried out using the system of equations (12). The computational mesh described in the previous section was used without any modifications. The general view of the computational domain (without buffer blocks) is shown in Fig. 3a.

The work [9] presents the results of calculations in the time domain in a nonlinear formulation, performed using the system of equations (1), (2). As part of this calculation, the discretized equations were directly solved for the given number of time steps using an explicit multirate Runge–Kutta scheme, which allows the use of different time steps in different parts of the computational domain. The calculation area in the circumferential direction had a size of 360°. The grid blocks for the nth interscapular passage of the row was obtained by duplicating the blocks of the zero interscapular passage of this row, followed by rotation to the required angle. The total size of the computational grid is 135 million cells. The diagram of the computational domain (without buffer blocks) is shown in Fig. 3b.

The advantage of this technique is that its use does not require the explicit formulation of assumptions about which interactions between the rows make a significant contribution to the noise of the turbomachine. All the interactions that the resolution of the computational grid used and the time step allow for modeling are taken into account in the calculation. At the same time, one has to put up with the extreme

resource intensity of this calculation method. It is difficult to consider it as a technique for performing routine calculations, but it can be used to obtain data for verification of less resource-intensive methods. In this study, the results of [9] are used precisely for this purpose.

10. DESCRIPTION OF THE CALCULATION PROCEDURE

The formulation of a nonstationary calculation in the method used begins with the determination of the harmonic fragments for which the calculation is planned to be carried out in each row. First of all, we should select the frequencies allowed in the rows. Circular frequencies of disturbances in this problem are specified using the following relations:

$$\omega^1 = (aB_1^2 + bB_2^2)\Omega, \quad |a| + |b| \le K_{\max}^1, \quad a, b \in \mathbb{Z}, \tag{14}$$

$$\omega^2 = (cB_1^1 + dB_2^1)\Omega, \quad |c| + |d| \le K_{\max}^2, \quad c, d \in \mathbb{Z}. \tag{15}$$

The azimuthal mode, which in the reference frame related to the stator, is described by frequency (14) for the given a and b, and in the reference frame related to the rotor by frequency (15) for the given c and d, is characterized in these reference systems by the azimuthal number

$$m = aB_1^2 + bB_2^2 + cB_1^1 + dB_2^1. \tag{16}$$

In this study, the values $K_{\max}^1$ and $K_{\max}^2$ are chosen to be equal to two. The analysis showed that in this case those modes that were dominant in the radiation according to the data of the previous calculations are resolved [6, 7]. A tone with a frequency of f_2 and simple combinations of tones f_1 and f_2 are obviously allowed. In addition, this choice of values of K_{max} makes it possible to take into account nonlinear interactions between modes to some extent, as shown in [10, 14]. It is easy to show that with such a choice of these values, in each row a calculation must be carried out for six nonzero frequencies, and for each frequency a calculation must be carried out for five harmonic fragments.

The number of harmonic fragments allowed in the first two rows can be somewhat reduced. Some of the harmonic fragments in these rows describe disturbances that, given the existing restrictions on the values of $K_{\max}$ due to the large absolute value m cannot propagate upstream (the cutoff effect for acoustic disturbances). They can be generated directly in these rows only due to nonlinear effects, which are assumed to be relatively weak for these disturbances. In the first row they are primarily disturbances for which $\mathrm{signum}(bB_2^2) = \mathrm{signum}(cB_1^1 + dB_2^1)$. In the second row they are the disturbances for which $\mathrm{signum}(aB_1^2 + bB_2^2) = \mathrm{signum}(dB_2^1)$. In this study, it was decided to neglect the contribution to the flow field from such disturbances. The analysis showed that in this case the number of harmonic fragments for which calculations must be carried out for each frequency in the first two rows can be reduced to three.

The computational domain containing three impeller passages for the first two rows and five impeller passages for the last two rows is presented (without buffer blocks) in Fig. 3c. The size of the computational grid is 13.6 million cells. It can be seen that the computational grid used within this method is still noticeably smaller than the computational grid for calculations in the time domain. At the boundaries located upstream and downstream of the computational domain, the characteristic boundary conditions were set in the calculation. The nonflow conditions were set on solid surfaces. The boundary conditions described by formula (13) were set at the outer boundaries of the computational domain, corresponding to the periodic boundaries of the impeller passages.

The unsteady flow field was calculated using the time-based method; 20000 steps were completed.

To illustrate the results obtained, Fig. 4 shows the fields of the logarithm of the amplitude of static pressure pulsations (normalized) for harmonics containing an azimuthal mode with $\omega = 86\ \Omega$ and $m = 15$ on cylindrical sections of the computational domain. It can be seen that in the rows belonging to the booster stage, the amplitudes of pressure pulsations differ significantly between the impeller passages, which indicates complex interactions inside the turbomachine. At the same time, in the fan impeller, the various impeller passages appear identical. It seems possible to reduce the number of passages for which calculations are carried out in blocks related to the fan impeller. Indeed, the numerical experiments have shown that the number of passages can be reduced to at least two without significantly changing the calculation results.

When the solution was established, a modal analysis of pulsations was carried out on the surface located at the entrance to the LPC. The surface on which the modal analysis was carried out is shown in Fig. 2 with a dashed line. The results of the modal analysis in the form of the powers allocated during the

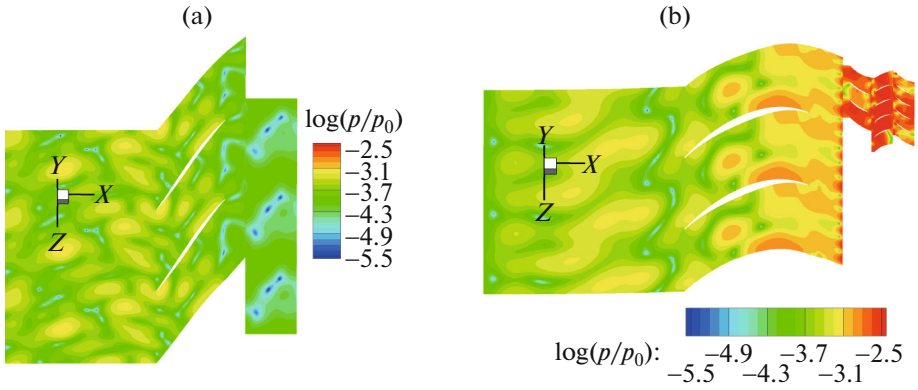

Fig. 4. Fields of the logarithm of the amplitude of static pressure pulsations for harmonics containing an azimuthal mode with $\omega = 86\ \Omega$, $m = 15$: (a) cylindrical section of the calculation area with diameter $d = 0.9\ D$; (b) cylindrical section of the calculation area with diameter $d = 0.53\ D$.

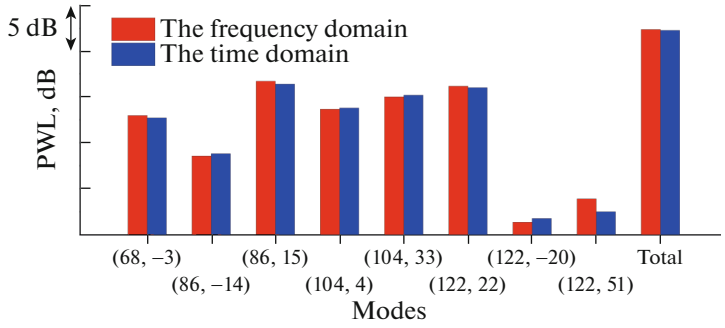

Fig. 5. The results of the modal analysis, presented in the form of azimuthal mode powers for harmonics with frequencies 68 Ω, 86 Ω, 104 Ω, 122 Ω.

analysis of the azimuthal modes corresponding to the acoustic disturbances propagating along the flow path are presented in Fig. 5. The modes are indicated by a pair of integers placed in parentheses, the first of which is j^2; and the second, m. Only modes with sound power levels less than 15 dB lower than the mode with the maximum sound power level are shown. Figure 5 also shows a comparison of the results of the modal analysis for the performed calculation with the results of the modal analysis for the time domain calculation presented in [9]. For all modes except the mode with $\omega = 122\ \Omega$ and $m = 51$, the difference between the powers of identical modes, according to the calculation results, is not more than 0.4 dB.

The results of the modal analysis were used to calculate the noise propagation through the air intake of the model stage. The calculation procedure and the geometry of the computational domain fully corresponded to those in [6–9]. To calculate noise propagation, linearized Euler equations were used for azimuthal modes in the frequency domain, specified on the meridional section of the air intake [16]. As a result of the calculation, pulsation fields in the near field of the air intake were obtained for all modes shown in Fig. 5. In turn, these data were used to calculate the pressure pulsations in the far field. They were calculated at points evenly spaced over an angle range of 1°–90° at 1° intervals on a circular arc of radius $r = 4$ m. The center of the arc was at the point of intersection of the surface passing through the vertices of the leading edges of the fan impeller blades and the axis of rotation of the low-pressure cascade shaft.

11. COMPARISON WITH EXPERIMENT

The results obtained were compared with the results of the experiment for the LPC under consideration carried out at the CIAM stand. In the front hemisphere, the experimental setup allows comparison for 12 microphones. The narrowband spectra obtained in the experiment were used as the initial data for

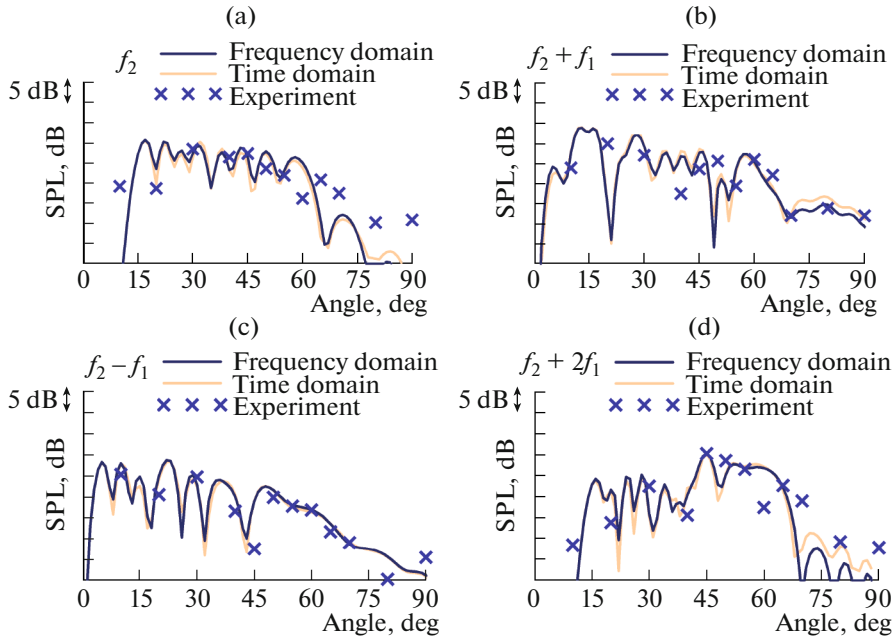

Fig. 6. Comparison of radiation patterns in the front hemisphere for calculated and experimental data: (a) f_2; (b) $f_2 + f_1$; (c) $f_2 - f_1$; (d) $f_2 + 2f_1$.

comparison, based on which radiation patterns for tonal noise were constructed for the desired harmonics.

The radiation patterns in the front hemisphere for the calculated and experimental data are presented in Fig. 6. The radiation patterns shown for frequencies $f_2 - f_1$, f_2, $f_2 + f_1$, and $f_2 + 2f_1$, obtained through this calculation, as well as the results of calculations in the time domain [9] and experimental data, are shown. In general, close agreement between the calculations can be seen. Satisfactory agreement is also observed between the calculation results and experiment.

12. CONCLUSIONS

This paper presents the results of computational studies of the tonal noise of the first booster stage of an LPC in the landing mode using the method for calculating the tonal noise of multistage turbomachines in the frequency domain developed at CIAM. For the first time, a version of the method is used for calculations in a three-dimensional setting that allows nonlinear effects to be taken into account. Another feature of this study is the use of the harmonic balance method for multitone disturbances with artificial frequency mapping when performing calculations. The calculation results are compared with the results of previously performed computational studies of the tonal noise of the given backup stage in the time domain (this calculation was also carried out in a nonlinear formulation). In addition, the calculation results were compared with the results of the experiment at the CIAM stand.

In general, the results of the calculations in the time and frequency domains are close to each other. In this case, closeness is observed both in the predicted modal composition of the radiation from the air intake and in the radiation patterns in the far field. In addition, for both calculations, satisfactory agreement is observed between the results of the calculation and experiment. Therefore, the results of this study can be considered as confirmation of the performance of the numerical method developed by the authors for calculating the tonal noise of multistage turbomachines in the frequency domain in a nonlinear formulation.

FUNDING

This work was supported by ongoing institutional funding. No additional grants to carry out or direct this particular research were obtained.

CONFLICT OF INTEREST

The authors of this work declare that they have no conflicts of interest.

REFERENCES

1. D. Broszat, D. Korte, U. Tapken, and M. Moser, "Validation of turbine noise prediction tools with acoustic rig measurements," in *15th AIAA/CEAS Aeroacoustics Conf. (30th AIAA Aeroacoustics Conf.), Miami, 2009* (American Institute of Aeronautics and Astronautics, 2009), pp. 2009–3283. https://doi.org/10.2514/6.2009-3283
2. N. Agarwal, U. Ganz, and J. Premo, "Compressor noise contribution to inlet noise," in *10th AIAA/CEAS Aeroacoustics Conf., Manchester, 2004* (American Institute of Aeronautics and Astronautics, 2004), pp. 2004–2913. https://doi.org/10.2514/6.2004-2913
3. L. Pinelli, F. Poli, M. Marconcini, A. Arnone, E. Spano, and D. Torzo, "Validation of a 3D linearized method for turbomachinery tone noise analysis," in *ASME 2011 Turbo Expo: Turbine Tech. Conf. and Exposition, Vol. 7: Turbomachinery, Parts A, B, and C, Vancouver* (ASMEDC, 2011), p. GT2011-45886. https://doi.org/10.1115/gt2011-45886
4. S. Vilmin, E. Lorrain, B. Tartinville, A. Capron, and C. Hirsch, "The nonlinear harmonic method: From single stage to multi-row effects," Int. J. Comput. Fluid Dyn. **27**, 88–99 (2013). https://doi.org/10.1080/10618562.2012.752074
5. A. A. Osipov and A. A. Rossikhin, "Calculation method for unsteady aerodynamic blade row interaction in a multistage turbomachine," TsAGI Sci. J. **45**, 255–271 (2014). https://doi.org/10.1615/tsagiscij.2014011921
6. A. Rossikhin, S. Pankov, and V. Mileshin, "Numerical investigation of the first booster stage tone noise of a high bypass ratio turbofan," in *ASME Turbo Expo 2016, Vol. 2A: Turbomachinery* (American Society of Mechanical Engineers, Seoul, South Korea, 2016), p. GT2016-57352. https://doi.org/10.1115/gt2016-57352
7. A. A. Rossikhin, S. V. Pankov, and V. I. Mileshin, "Numerical and experimental investigation of the first booster stage tone noise at different operational conditions," in *Proc. of the 15th Int. Symp. on Unsteady Aerodynamics, Aeroacoustics and Aeroelasticity of Turbomachines* (Central Institute of Aviation Motors, Oxford, 2018), pp. 24–27.
8. A. Rossikhin, S. Pankov, and V. Mileshin, "Numerical investigation of the low pressure compressor tone noise of a high bypass ratio turbofan," in *ASME Turbo Expo 2020, Vol. 2D: Turbomachinery* (American Society of Mechanical Engineers, London, UK, 2020), p. GT2020-14897. https://doi.org/10.1115/gt2020-14897
9. V. Mileshin, S. Pankov, and A. Rossikhin, "Numerical and experimental investigation of the turbofan first booster stage tone noise," in *Proc. 23rd Int. Congress on Acoustics* (Aachen, Germany, 2019), pp. 1608–1615. https://doi.org/10.1115/gt2016-57352
10. A. A. Rossikhin, "Frequency-domain method for multistage turbomachine tone noise calculation," Int. J. Aeroacoustics **16**, 491–506 (2017). https://doi.org/10.1177/1475472x17730458
11. L. He, "Fourier modeling of steady and unsteady nonaxisymmetrical flows," J. Propulsion Power **22**, 197–201 (2006). https://doi.org/10.2514/1.15701
12. S. C. Stapelfeldt and L. Di Mare, "Reduced passage method for multirow forced response computations," AIAA J. **53**, 3049–3062 (2015). https://doi.org/10.2514/1.j053888
13. E. Gad, *Simulation of RF Integrated Circuits* (Univ. of Ottawa, Ottawa, 2007).
14. A. A. Rossikhin and V. I. Mileshin, "Application of the 2.5D harmonic balance method to calculate the propagation of unsteady disturbances through a duct of a turbofan," Math. Models Comput. Simul. **14**, 129–138 (2022). https://doi.org/10.1134/s2070048222010185
15. M. Nyukhtikiv, I. Brailko, V. Mileshin, and S. Pankov, "Computational and experimental investigation of unsteady and acoustic characteristics of counter-rotating fans," in *Proc. of 2004 ASME Heat Transfer, Fluids Engineering Summer Conference, Charlotte, N.C., 2004* (ASME, 2004), Vol. 2, pp. 871–879. https://doi.org/10.1115/HT-FED2004-56435
16. M. A. Nyukhtikov, A. A. Rossikhin, V. V. Sgadlev, and I. A. Brailko, "Numerical method for turbomachinery tonal noise generation and radiation simulation using CAA approach," in *ASME Turbo Expo 2008: Power for Land, Sea, and Air, Vol. 6: Turbomachinery, Parts A, B, and C, Berlin, 2008* (ASME, 2008), p. GT2008-51182. https://doi.org/10.1115/gt2008-51182

17. M. McMullen, A. Jameson, and J. Alonso, "Application of a non-linear frequency domain solver to the Euler and Navier–Stokes equations," in *AIAA 40th Aerospace Sci. Meeting* (American Institute of Aeronautics and Astronautics, Reno, Nev., 2002, 2002), p. 2010-0120.
https://doi.org/10.2514/6.2002-120
18. C. K. W. Tam and J. C. Webb, "Dispersion-relation-preserving finite difference schemes for computational acoustics," J. Comput. Phys. **107**, 262–281 (1993).
https://doi.org/10.1006/jcph.1993.1142
19. V. Allampalli, R. Hixon, M. Nallasamy, and S. D. Sawyer, "High-accuracy large-step explicit Runge–Kutta (HALE-RK) schemes for computational aeroacoustics," J. Comput. Phys. **228**, 3837–3850 (2009).
https://doi.org/10.1016/j.jcp.2009.02.015
20. A. Jameson, W. Schmidt, and E. Turkel, "Numerical solution of the Euler equations by finite volume methods using Runge Kutta time stepping schemes," in *14th Fluid and Plasma Dynamics Conf., Palo Alto, Calif., 1981* (American Institute of Aeronautics and Astronautics, 1981), p. 1981-1259.
https://doi.org/10.2514/6.1981-1259
21. M. B. Giles, "Nonreflecting boundary conditions for Euler equation calculations," AIAA J. **28**, 2050–2058 (1990).
https://doi.org/10.2514/3.10521
22. J. E. Ffowcs Williams and D. L. Hawkings, "Sound generation by turbulence and surfaces in arbitrary motion," Philos. Trans. R. Soc. London, Ser. A: Math. Phys. Sci. **264**, 321–342 (1969).
https://doi.org/10.1098/rsta.1969.0031